ORAL/POSTER REFERENCE:

EFFECT OF FIBER COATINGS ON DETECTION OF TRANSVERSE CRACKS IN CFRP COMPOSITES USING FBG SENSORS

Y. Okabe, N. Tanaka, T. Mizutani, S. Yashiro, and N. Takeda

Graduate School of Frontier Sciences, The University of Tokyo
c/o Takeda Lab., Komaba Open Laboratories, The University of Tokyo,
4-6-1 Komaba, Meguro-ku, Tokyo 153-8904, JAPAN

ABSTRACT

FBG sensors have been applied to the detection of transverse cracks in CFRP cross-ply laminates using the sensitivity of the sensors to non-uniform strain distribution. However, there is the possibility that the resin coating of the FBG sensors will relax the non-uniform strain distribution and deteriorate the sensitivity of the sensors. Hence, in this study, the strain transfer from the 0° ply to the core of the optical fiber was calculated by a theory developed from the shear-lag model. As a result, it was found that the variation of axial strain in the core of a polyimide-coated FBG sensor was smaller than that of an uncoated FBG sensor. Nevertheless, the reflection spectra of the coated and uncoated FBG sensors calculated from the strain distributions were almost the same. This result shows that the coating of the optical fiber does not deteriorate the sensitivity of the FBG sensor for the detection of transverse cracks, and the coated FBG sensors can be used without removal of the fiber coatings.

KEYWORDS

Fiber Bragg grating sensor, CFRP, transverse crack, strain distribution, resin coating, shear-lag model.

INTRODUCTION

The authors have applied FBG sensors to the detection of transverse cracks in CFRP cross-ply laminates [1]. When transverse cracks appear in 90° ply under tensile loading, the longitudinal strain distribution in 0° ply becomes non-uniform. Since an FBG sensor is embedded in 0° ply, the reflection spectrum of the FBG sensor is distorted by the non-uniform strain distribution. Thus, the occurrence of transverse cracks can be detected from the change in the form of the reflection spectrum.

With regard to the application of this technique for practical use, the optical fibers without resin coatings have problems in handling for embedding, and the durability of the fibers is lower than that of coated optical fibers. Hence optical fibers coated with polyimide should be used. However, the coating relaxes the non-uniform strain distribution transferred from the 0° ply to the optical fiber, because the stiffness of the coating is much smaller than that of the glass optical fiber. This effect may decrease the sensitivity of the FBG sensor. Hence, in this research, the strain transfer from the 0° ply to the core of the optical fiber was calculated by a theory developed from the shear-lag model, and the effect of the fiber coating on detection of transverse cracks was

investigated.

STRAIN DISTRIBUTION IN 0° PLY OF A CFRP CROSS-PLY LAMINATE

The FBG sensor has been embedded in 0° ply on the border of 90° ply in a CFRP cross-ply laminates for the detection of transverse cracks that run through the thickness and width of the 90° ply, as shown in Figure 1(a) [1]. The occurrence of the transverse cracks can be detected from the change in the form of the reflection spectrum from the FBG sensor owing to the non-uniform strain distribution. Hence, the longitudinal strain distribution in 0° ply was calculated theoretically. As shown in Figure 1, McCartney's theory [2] was applied for each region between two neighboring cracks. In this analysis, generalized plane strain conditions are assumed, and calculated longitudinal strains in 0° ply are the values averaged through the thickness of the 0° ply.

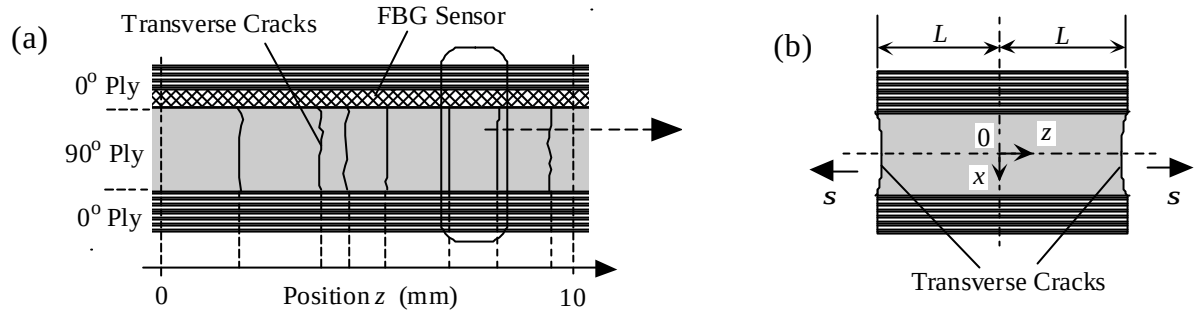

Figure 1: Schematic diagram for the calculation of the non-uniform strain distribution caused by transverse cracks: (a) positions of transverse cracks obtained from an experiment; (b) a region between two neighboring cracks where McCartney's theory is applied.

STRAIN TRANSFER TO THE CORE OF AN OPTICAL FIBER

Duck et. al. proposed a derivation that could predict the axial strain field of an embedded optical fiber sensor from a given arbitrary varying axial strain field in the surrounding material [3]. From the calculation results, they indicated that the in-fiber strain could not be assumed to be equal to the strain field present in the surrounding material. In this research, we modified the method to apply to multiple cylinder models and calculate the strain transfer more accurately.

The optical fiber coated with resin is assumed to be axisymmetric and divided into thin concentric cylindrical layers. The layers are numbered from the innermost core, so that the *i*th cylinder occupies the region $r_{i-1} \le r \le r_i$ for $i = 1 \ldots N$, where r_i denotes the outer radius of the *i*th cylinder and $r_0 = 0$. Figure 2(a) shows a free-body diagram of the *i*th layer. Since the radial and azimuthal stresses are assumed to be negligible, equilibrium equation is expressed as follows:

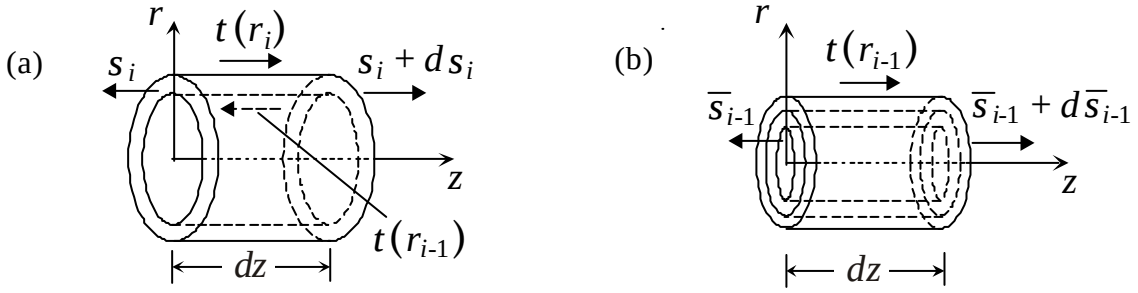

Figure 2: Free-body diagrams of a multiple cylinder model: (a) the *i*th layer; (b) the inner cylinder assembly of the *i*th layer.

$$\frac{\partial \sigma_i(z)}{\partial z}\pi\left(r_i^2 - r_{i-1}^2\right) + \tau(r_i, z)2\pi r_i - \tau(r_{i-1}, z)2\pi r_{i-1} = 0 \tag{1}$$

Figure 2(b) shows the inner cylinder assembly of the ith layer, where $\bar{\sigma}_{i-1}$ denotes the mean normal stress averaged over i-1 inner layers:

$$\bar{\sigma}_{i-1} = \sum_{j=1}^{i-1} E_j \varepsilon_j \frac{r_j^2 - r_{j-1}^2}{r_{i-1}^2} \tag{2}$$

Hence, the relationship of the stresses acting on the inner cylinder assembly is given by

$$\frac{\partial \bar{\sigma}_{i-1}(z)}{\partial z}\pi r_{i-1}^2 + \tau(r_{i-1}, z)2\pi r_{i-1} = 0 \tag{3}$$

The shear stress is expressed by

$$\tau(r, z) = G\left(\frac{\partial w(r, z)}{\partial r} + \frac{\partial u(r, z)}{\partial z}\right) \cong G\frac{\partial w(r, z)}{\partial r} \tag{4}$$

where u and w are displacements along r and z, respectively. From the Eqn.s 1-4, the following equation is obtained.

$$2G_i\left[\varepsilon_i(r_i, z) - \varepsilon_{i-1}(r_{i-1}, z)\right] + E_i\left[\frac{r_i^2 - r_{i-1}^2}{2} - r_{i-1}^2 \ln\left(\frac{r_i}{r_{i-1}}\right)\right]\frac{\partial^2 \varepsilon_i(r_i, z)}{\partial z^2} + \sum_{j=1}^{i-1} E_j\left(r_j^2 - r_{j-1}^2\right)\ln\left(\frac{r_i}{r_{i-1}}\right)\frac{\partial^2 \varepsilon_j(r_j, z)}{\partial z^2} = 0 \tag{5}$$

Then, the Fourier transform of $\varepsilon_i(r_i, z)$ is symbolized by $\hat{\varepsilon}_i(r_i, k)$, and $\hat{\varepsilon}_i(r_i, k)$ is related to $\hat{\varepsilon}_1(r_1, k)$ using a transfer function $H_i(k)$ as $\hat{\varepsilon}_i(r_i, k) = H_i(k)\hat{\varepsilon}_1(r_1, k)$. The Fourier transform of Eqn. 5 yields

$$\hat{\varepsilon}_i(r_i, k) = \frac{2G_i H_{i-1}(k) + \sum_{j=1}^{i-1}(2\pi k)^2 E_j H_j(k)\left(r_j^2 - r_{j-1}^2\right)\ln(r_i / r_{i-1})}{2G_i - (2\pi k)^2 E_i\left[\left(r_i^2 - r_{i-1}^2\right)/2 - r_{i-1}^2 \ln(r_i / r_{i-1})\right]}\hat{\varepsilon}_1(r_1, k) \tag{6}$$

Thus, $H_i(k)$ is expressed using the transfer functions $H_j(k)$ (j = 1…i-1). At first, $H_2(k)$ is obtained from $H_1(k)$ = 1. Next, $H_3(k)$ is calculated from the $H_2(k)$ and $H_1(k)$. Through the repetition of the calculation procedure, all $H_i(k)$ (i = 1…N) are obtained at discrete values of k.

From a given strain field at the outermost layer $\varepsilon_N(r_N, z)$, $\hat{\varepsilon}_N(r_N, k)$ is obtained by the Fourier transform. Then $\hat{\varepsilon}_1(r_1, k)$ is calculated from the $\hat{\varepsilon}_N(r_N, k)$ using the $H_N(k)$, and the strain field at the innermost core $\varepsilon_1(r_1, z)$ can be obtained by the inverse Fourier transform.

CALCULATION OF REFLECTION SPECTRA

According to the above procedure, axial strain distribution at the core of the FBG sensor embedded in a CFRP laminate was calculated. The CFRP laminate is T800H/3631 (Toray Industries, Inc), and the laminate configuration is cross-ply [0_2/90_4/0_2]. The optical fiber is made from glass whose Young's modulus is 73.1 GPa and whose Poisson's ratio is 0.16. The core and cladding are 10 μm and 125 μm in diameter, respectively. The length of the grating is 10 mm, and the grating period is about 530 nm. Strain distribution was calculated for an uncoated FBG sensor and an FBG sensor coated with polyimide, whose outside diameter was 150 μm. Young's

modulus and Poisson's ratio of the polyimide are 1.47 GPa and 0.45, respectively. In the analysis, the glass optical fiber was divided into seven concentric cylinders, and the polyimide coating into two cylinders.

Figure 3 shows the longitudinal strain distribution in 0° ply calculated from the positions of transverse cracks in Figure 1(a) obtained from a tensile test. The average tensile stress was 359 MPa. Furthermore, axial strain distributions at the cores of uncoated and polyimide-coated FBG sensors are shown in Figure 3. In the calculation, the strain distribution at the outermost layer was assumed to be the same as that in 0° ply. As shown in Figure 3, although the strain distribution in the uncoated FBG sensor scarcely changed from that in 0° ply, the variation of the strain in the polyimide-coated FBG sensor was attenuated and smoothed because of the soft coating.

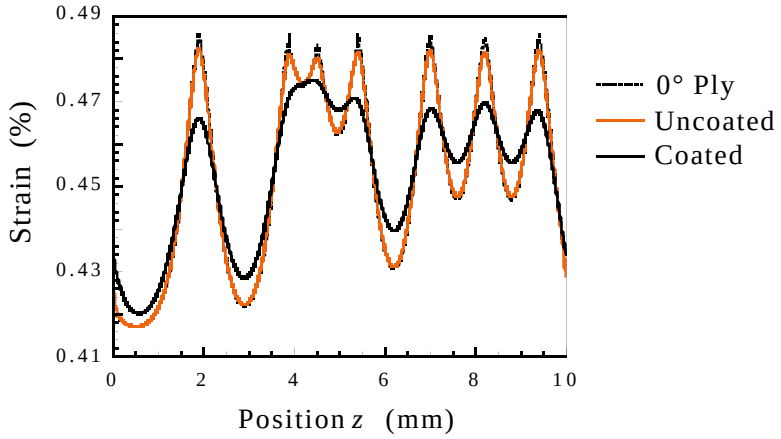

Figure 3: Longitudinal strain distribution in 0° ply calculated from the positions of transverse cracks in Figure 1(a) and axial strain distributions calculated at the cores of uncoated and polyimide-coated FBG sensors. The average tensile stress was 359 MPa.

From the axial strains, the distributions of the grating period and the average refractive index along the FBG sensors were calculated. Then, the reflection spectra were simulated from the distributions. This calculation was conducted using the software 'IFO_Gratings' developed by the Optiwave Corporation. This program can calculate the spectrum by solving the couple mode equations using the transfer matrix method. The reflection spectra calculated from the strain distributions in Figure 3 are shown in Figure 4. The deformation of the spectrum of the coated FBG sensor is slightly smaller than that of the uncoated FBG sensor. Peaks and dips of strain distribution in Figure 3 correspond to large wavelength and small wavelength components of the spectrum, respectively. Thus, the relaxation of the non-uniform strain distribution by the polyimide coating affects the intensity of the components away from the center wavelength of the reflection spectrum. However, the two spectra in Figure 4 are almost the same, so that the polyimide-coated FBG sensor can be applied to the detection

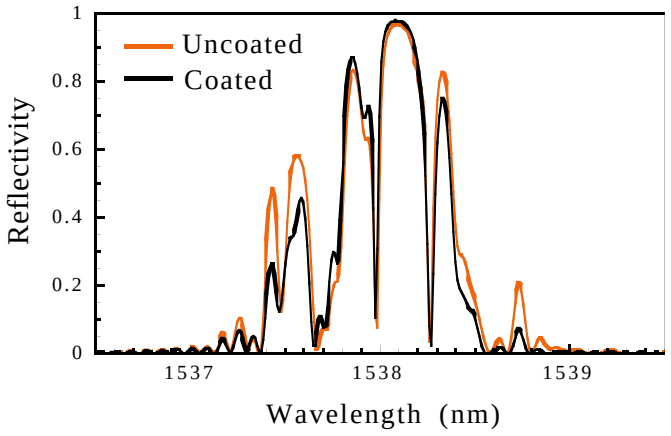

Figure 4: The reflection spectra of the uncoated and coated FBG sensors calculated from the strain distributions in Figure 3.

of transverse cracks. The agreement of the spectra between coated and uncoated FBG sensors were confirmed also in the cases that the crack density was very small or saturated, from theoretical calculations.

CONCLUSIONS

In this research, Duck's method was modified to be applied to multiple cylinder models and calculate the strain transfer from a surrounding material to the core of an optical fiber more accurately. From the analysis, it was found that the polyimide coating of an optical fiber relaxed the non-uniform strain distribution caused by the occurrence of transverse cracks in CFRP laminates. However, the reflection spectrum of a polyimide-coated FBG sensor, which was calculated from the relaxed strain distribution, was almost the same as that of an uncoated FBG sensor. Thus, the polyimide-coated FBG sensor can be applied to the detection of transverse cracks without removal of the fiber coating.

ACKNOWLEDGEMENTS

This research was conducted as a part of the 'R&D for Smart Materials Structure System' project within the Academic Institutions Centered Program supported by NEDO (New Energy and Industrial Technology Development Organization), Japan.

REFERENCES

1. Okabe, Y., Yashiro, S., Kosaka, T., and Takeda, N. (2000) *Smart Mater. Struct.* 9, 832.
2. McCartney, L.N. (1992) *J. Mech. Phys. Solids* 40, 27.
3. Duck, G. and LeBlanc, M. (2000) *Smart Mater. Struct.* 9, 492.